Central nervous system infusion of TrkB agonist, 7,8-dihydroxyflavone, is ineffective in promoting myelin repair in cuprizone and experimental autoimmune encephalomyelitis mouse models of multiple sclerosis

List title: 7,8-dihyroxyflavone in preclinical MS mouse models

Authors: Jessica L Fletcher[1,2*], Rhiannon J Wood[1], Alexa R Prawdiuk[1], Ryan O'Rafferty[1], Ophelia Ehrlich[1], David G Gonsalvez[1,3], and Simon S Murray[1*]

[1]Department of Anatomy & Physiology School of Biomedical Sciences, Faculty of Medicine, Dentistry & Health Sciences, University of Melbourne, VIC, Australia

Present address:

[2]Menzies Institute for Medical Research, University of Tasmania, Hobart, TAS, Australia.

[3]Department of Anatomy and Developmental Biology, School of Biomedical Sciences, Monash University, VIC, Australia

***Corresponding author(s):**
Email: jessica.fletcher@utas.edu.au (JLF), Email: ssmurray@unimelb.edu.au (SSM)

CRediT author contributions: Jessica Fletcher: conceptualization, data curation, formal analysis, investigation, project administration, supervision, visualization, writing – original draft preparation. Rhiannon Wood: investigation, methodology, project administration, validation, writing – review & editing. Alexa Prawdiuk: investigation. Ryan O'Rafferty: investigation. Ophelia Ehrlich: investigation. David Gonsalvez: methodology, resources, validation, writing – review & editing. Simon Murray: conceptualization, funding acquisition, project administration, resources, supervision, writing – review & editing.

Abstract

Small molecular weight functional mimetics of brain-derived neurotrophic factor (BDNF) which act via the TrkB receptor have been developed to overcome the pharmacokinetic limitations of BDNF as a therapeutic agent for neurological disease. Activation of TrkB signalling on oligodendrocytes has been identified as a potential strategy for promoting myelin repair in demyelinating conditions such as Multiple Sclerosis (MS). Here, we tested the efficacy of intracerebroventricular infusion of TrkB agonist 7,8-dihydroxyflavone (DHF) to promote myelin repair in the cuprizone model of de- and remyelination and alter the course of experimental autoimmune encephalomyelitis (EAE), after the onset of clinical signs. In these two distinct, but common mouse models used for the preclinical testing of MS therapeutics, we found that DHF infusion increased the percentage of myelin basic protein and density of oligodendrocyte progenitor cells (OPCs) in the corpus callosum of female C57BL/6 mice after cuprizone demyelination. However, DHF did not alter the percentage of axons myelinated or increase the density of post-mitotic oligodendrocytes in this model. Direct central nervous system infusion of DHF infusion also had no effect on the clinical course of EAE in male and female C57BL/6 mice, and examination of the lumbar spinal cord after 21 days of treatment revealed extensive demyelination, with active phagocytosis of myelin debris by Iba1+ macrophages/microglia. These results indicate that direct central nervous system infusion of DHF is ineffective at promoting myelin repair in toxin-induced and inflammatory models of demyelination.

Keywords: TrkB, oligodendroglia, multiple sclerosis, experimental autoimmune encephalomyelitis, cuprizone

Introduction

Neurotrophins have long been identified as therapeutic candidates to treat neurologic disorders due to their ability to promote neuronal survival and differentiation as well as synaptic plasticity (1). However, it is only comparatively recently that the effects neurotrophins mediate *via* glial cells have received attention as a potential mechanism to prevent neurodegeneration (2,3). This includes the effect of brain-derived neurotrophic factor (BDNF), which has been shown to promote central nervous system (CNS) myelination via its TrkB receptor (4,5). That BDNF elicits oligodendroglial differentiation and myelination by activating TrkB is highly relevant for the auto-immune demyelinating disease, multiple sclerosis (MS). Although there are now many immune-targeted therapies that can significantly modify the course of relapsing-remitting MS, there are no treatments which can prevent or reverse the axon loss and neuron death that lead to the increasing severity of neurologic dysfunction experienced by patients with progressive MS (6,7). Therefore, neuroprotective therapeutic strategies that can also promote myelin repair—such as selectively targeting the TrkB receptor—are highly sought-after as adjunct treatments to the immuno-modulatory therapies clinically available for MS.

Although attractive as a remyelinating therapeutic, BDNF itself has poor pharmacokinetic properties – it is a large molecule unable to cross the blood-brain barrier, that is rapidly cleared systemically (8) and is non-selective, interacting with both TrkB and the pan-neurotrophin receptor $p75^{NTR}$ (1,2,9). Collectively, these properties of BDNF have led to the development of multiple smaller molecular weight TrkB agonists, also called functional BDNF-mimetics (1,10–12). This includes TDP6 and LM22A-4, both which promote myelin repair in an oligodendroglial TrkB-dependent manner in the cuprizone model of de- and remyelination, in which MS therapies for myelin repair are frequently tested (13,14). Notably, 7,8-dihydroxyflavone (DHF), the most widely used TrkB agonist within the biomedical literature (Fig. S1) has

not previously been tested in cuprizone. However, in the experimental autoimmune encephalomyelitis (EAE) animal model for MS it has been shown to significantly reduce the course of clinical signs when administered prophylactically via intra-peritoneal injection (15). In addition, DHF has undergone extensive biochemical and biophysical characterisation to demonstrate its ability to interact with the extracellular domain of TrkB and elicit TrkB phosphorylation *in vitro* (16). As a flavonoid, DHF has also been shown to act as an anti-oxidant, promoting survival in neuronal cell culture models of oxidative stress independent of TrkB receptor expression (17,18). Overall, the ability of DHF to elicit TrkB signalling and act as a neuroprotective anti-oxidant makes it a promising candidate to promote myelin repair in the context of MS and inflammatory demyelination.

To test the capacity of DHF to promote myelin repair in response to inflammatory demyelination, two mouse models of myelin loss were used, the cuprizone model and EAE. In the toxin-induced cuprizone model, mature oligodendrocytes are selectively killed resulting in profound demyelination and inflammatory gliosis, followed by rapid remyelination once cuprizone is withdrawn (13,14,19). In this respect, the cuprizone model is superior to the immune-mediated EAE model, as myelin repair occurs stereotypically, and can be quantified. However, it does not mimic the auto-immune attack against myelin which characterises MS. This is achieved in the EAE model, in which mice are immunised against a myelin protein (typically myelin oligodendrocyte glycoprotein, MOG), which results in neuroinflammation and clinical signs of ascending paralysis, but determining if remyelination has occurred in EAE is challenging (20). In the current study DHF was administered directly to the CNS via intracerebroventricular infusion into the cerebrospinal fluid in both models. This was done to enable direct comparison with previous cuprizone studies investigating the remyelinating potential of TrkB activation (13,14), and to limit possible modulation of the peripheral immune system. In addition, in EAE, DHF was administered at the onset of clinical signs to more closely reflect MS patient treatment following initial clinical presentation.

Materials & Methods

Experimental animals

Male and female C57BL/6 mice, aged 6-7-weeks old were purchased from the Animal Resource Centre (Perth, Australia) and group housed in specific pathogen-free conditions at the Melbourne Brain Centre Animal Facility, under a 12 hour light / dark cycle with *ad libitum* access to food and water. Animals were habituated to the new housing environment for a minimum of 7 days. All procedures were performed with approval from the Florey Institute of Mental Health and Neuroscience Animal Ethics Committee (#12-042, #18-024) and followed the Australian Code of Practice for the Care and Use of Animals for Scientific Purposes.

Cuprizone-induced demyelination

At 8 weeks of age, female mice were fed 0.2% cuprizone in normal chow (Teklad Custom Diets) for 6-weeks to induce demyelination. Cuprizone was then removed, and mice were killed (*n*=2/cohort) or underwent intracerebroventricular pump implantation to receive aCSF, DMSO vehicle or DHF for 7 days. Only female mice were used in cuprizone experiments due to the increased incidence of MS in females (21).

Experimental autoimmune encephalomyelitis and clinical monitoring

To induce experimental autoimmune encephalomyelitis (EAE), male and female mice, aged 8 weeks received subcutaneous injections to both flanks and base of the tail of MOG_{35-55} peptide (125µg total, Mimotopes) emulsified 1:1 (vol/vol) in Freund's complete adjuvant (BD Cat# 263810) containing additional *Mycobacterium tuberculosis* (5mg/mL, BD Cat# 231141). This was followed by intraperitoneal injection of 400ng pertussis toxin (List Biological Laboratories, Sapphire Biosciences Cat# 70323-44-3) in 0.1mL in sterile phosphate buffered saline (PBS). Mice were anaesthetized for all injections on Day 0 with

exposure to 4% isoflurane in air which was maintained for less than 5 mins at 0.5-1.5% isoflurane through a nose cone. On Day 3, all mice received a second intraperitoneal injection of 400ng pertussis toxin. Mice were weighed and assessed for EAE clinical signs daily. EAE clinical scores was graded according to Table 1.

Table 1: Scoring criteria for daily assessment of clinical signs in EAE mice.

Score	Description
0	Normal appearance, tail lifts and normal gait.
1	Normal gait, but tail is weak and is slow or fails to curl around finger when stroked.
1.5	Tail is weak, is slow / fails to curl around finger when stroked. Normal appearing gait, but some hindlimb weakness when performing hindlimb clasp test (22).
2.0	Complete tail paralysis, can no longer be lifted by mouse and fails to curl around finger when stroked.
2.25	Complete tail paralysis and some hindlimb weakness when performing hindlimb clasp test.
2.5	Complete tail paralysis and hindlimb weakness when performing hindlimb clasp test.
2.75	Complete tail paralysis and paralysis of one hindlimb when walking.
3.0	Complete tail and hindlimb paralysis, but maintains righting reflex, when placed on back / side.
3.5	Complete tail and hindlimb paralysis, with forelimb weakness and loss of righting reflex or signs of urinary / faecal incontinence. Requires immediate euthanasia.
4.0	Spontaneous death.

Intracerebroventricular delivery of 7,8-dihydroxyflavone (DHF)

Cuprizone and EAE mice received intracerebroventricular (ICV) osmotic minipumps (Azlet) vehicle as previously described (13) of 762ng/day 7,8-dihydroxyflavone (equivalent to 250µM for the 7 day infusion with 0.5µL/hr flowrate, or 500µM for the 21 day infusion with 0.25µL/hr flowrate, DHF), artificial aCSF (cuprizone mice only) or 14% (v/v) DMSO. DHF doses were based on previous *in vitro* studies, wherein 250-500nM of DHF was required to reach the same level of neuronal survival as BDNF (12). Briefly, mice were anaesthetised with 2-4% isoflurane in normal air, scalp was shaved, and mice were fitted into a stereotaxic frame receiving 1.5-2.5% isoflurane in air via a nose cone. A sagittal incision was made across the midline of the scalp, and a 1.5mm burr hole was made at +0.5mm rostral and -0.7mm lateral from

Bregma using a microdrill. Reservoirs were placed subcutaneously along the flank and cannulae were implanted and fixed in place using an ethyl cyanoacrylate adhesive (Loctite). Vicyrl sutures (Ethicon, Cat# J492G) were used to close head wounds and animals placed in recovery chamber at 32°C and closely monitored until ambulatory, before being single-housed in standard cages (Technoplast). Cuprizone treated mice received 7-day pumps (Azlet #1007D) on the final day of cuprizone exposure before being returned to normal chow and tolerated the procedure well. EAE mice received 28-day pumps (Azlet #2004) on Day 13 if they demonstrated tail weakness or tail paralysis. Of 19 EAE mice that underwent the procedure 10 either died due to anaesthetic complications or were excluded due to poor wound healing. One EAE-induced mouse did not develop clinical signs by Day 13 and was excluded. Due to high mortality and exclusion rate, ICV implantation in EAE mice was discontinued.

Tissue collection, processing, and immunofluorescence

All mice were anaesthetised with isoflurane and euthanased with barbiturates (Lethabarb, Vibrac Australia) before transcardial perfusion with sterile 0.1M PBS, then ice-cold 4% paraformaldehyde (PFA). Brains from cuprizone mice and the lumbar enlargement of spinal cords from EAE mice were removed. Tissues were post-fixed overnight in 4% PFA, then washed in 0.1M PBS and cryoprotected in 30% sucrose. For electron microscopy (EM) studies of cuprizone mice, the first millimeter of the right hemisphere from the sagittal midline was selected and placed in Kanovsky's buffer overnight and washed in 0.1M sodium cacodylate before resin embedding at the Centre for Advanced Histology and Microscopy at the Peter MacCallum Centre. Remaining cuprizone brain tissue was oriented sagittally, while EAE spinal cords were oriented longitudinally for embedding in OCT (Tissue-tek) and frozen in isopentane over dry ice. Tissue blocks were stored at -80°C until sectioning at 16µm (brain) or 20µm (spinal cord) using a cryostat maintained at -16 to -17°C, with sections collected on Superfrost^{+} slides. Slides were air-dried and stored

153 at -80°C before use. Approximately 70-100 µm separated adjacent sections on the same slide and sagittal
154 brain sections cut beyond ± 2.64mm from the lateral midline were excluded as previously (13,14)

155

156 Primary antibodies for immunostaining are listed in Table 2. Slides were immersed in three exchanges of
157 0.1M PBS, before overnight incubation at room temperature with primary antibodies diluted in 10%
158 normal donkey serum (NDS) with 0.3% Triton-X 100 in 0.1M PBS. Next, slides were washed three times in
159 0.1M PBS before incubation with appropriate AlexaFluor-conjugated secondary antibodies
160 (ThermoFisher) for 2 hours at room temperature, after which slides underwent a final wash and were
161 cover slipped using aqueous mounting solution (Dako). After air-drying slides were stored at 4°C until
162 imaging. Modifications for MBP staining included immersing slides in ice-cold 100% methanol for 10mins
163 prior first wash. When used, Hoeschst33342 (ThermoFisher) was the nuclear counterstain.

164 **Table 2: Antibodies used for immunostaining**

Antibody	Maker for	Manufacturer	RRID	Concentration Used
Monoclonal rat anti-MBP	Myelin basic protein	Millipore (MAB386)	AB_9497	1:200
Polyclonal rabbit anti-Olig2	Oligodendrocyte lineage	Millipore (AB9610)	AB_570666	1:200
Polyclonal goat anti-PDGFRα	Oligodendrocyte progenitor cell	R&D Systems (AF1062)	AB_2236897	1:200
Monoclonal mouse anti-CC1	Post-mitotic oligodendrocyte	Millipore (OP-80)	AB_2057371	1:200
Polyclonal goat anti-Iba1	Macrophages/microglia	Abcam (ab5076)	AB_22244	1:200

165

166 *Fluorescence imaging and analysis*

167 All imaging was performed blinded to treatment group. For sagittal sections, imaging was restricted to
168 the caudal region of the corpus callosum approximately -1.1mm to -3.0mm from Bregma, and tracts

169 contributing to the dorsal hippocampal commissure were excluded as previously (13). Spinal cord sections
170 were from approximately L2 to S1, with imaging restricted to the lateral white matter tracts. For each
171 analysis, a minimum of three sections per animal were imaged.

172

173 MBP staining was imaged under a 20x (0.8 NA) lens using an RGB camera (AxioVision Hr, Zeiss) attached
174 to an epifluorescence Axioplan2 Imager (Zeiss) microscope using consistent exposure times. All remaining
175 stains were imaged using Zeiss LSM510 Meta, LSM780 or LSM880 confocal microscope with 405nm,
176 488nm, 561nm or 633nm laser lines. Images acquired on the LMS780 and 880 were processed (tiles
177 stitched, and maximum z-projections produced) using Zen Black software. Uniform acquisition settings
178 were used for each staining batch. Brightness and contrast were adjusted if needed for counting and
179 presentation purposes.

180

181 Oligodendroglial cell counts were performed manually as described in (14) using FIIJ/Image J and
182 expressed as number of cells/mm^2.

183

184 *Electron microscopy and analysis*

185 Electron microscopy and analysis was performed as described in (13). Briefly, after region selection on
186 semi-thin sections collected on glass slides and stained with 1% toluidine blue, ultrathin sections were
187 collected on 3mm x 3mm copper grids and examined using a JEOL 1011 transmission electron microscope,
188 and imaged using a MegaView III CCD cooled camera operated with iTEM AnalySIS software (Olympus
189 Soft Imaging Systems). A minimum of six distinct fields of view were captured at 10 000x magnification
190 per animal, and used to count myelinated axons in FIJI/Image J. For this analysis, DHF treated animals

were compared to animals that solely received aCSF vehicle treated animals previously published in (13,14) as DMSO treated animals were not processed for EM analyses. Sectioning, post-staining and EM imaging were all performed at the Centre for Advanced Histology and Microscopy, Peter MacCallum Centre.

Spectral confocal reflectance (SCoRe) microscopy

SCoRe microscopy on longitudinally oriented spinal cord from EAE mice was performed as described in (23), and combined with fluoromyelin (ThermoFisher Cat# F34652, RRID: AB_2572213) and Iba1 immunostaining. Briefly, before imaging sections were washed in 0.1M PBS and incubated at 4°C with goat-anti Iba1 (Table 2) in 10% NDS without 100% Triton-X 100 to keep myelin membranes intact for 2 nights in a humified chamber. Sections were washed and incubated with donkey anti-goat AlexaFluor488 for 4 hours at room temperature, before being washed and then incubated in 50% fluoromyelin in PBS for 20 min, and washed thoroughly, before being mounted with #1.5 coverslips (Zeiss, 1.5H, 170±5µm). SCoRe images were captured using a Zeiss LSM880 confocal microscope using 40x oil immersion lens (1.3 NA) and immersion oil (Zeiss, Immersol 518F), with a refractive index of 1.518. Closely, matched refractive index of the coverslip and immersion oil prevented reflection of light from the glass coverslip interfering with SCoRe signal. Lasers with 488nm, 561nm and 633nm wavelengths were passed through acousto-optical tunable filters (AOTF) 488-640 filter/splitter and a 20/80 partially reflective mirror. Reflected light was collected using three photodetectors set to collect light through narrow bands defined by prism and mirror slides, centred around the laser wavelengths.

Experimental design and statistical analyses

All quantitative assessments were performed by an observer blinded to animal and treatment identity with a minimum of 3 animals per group assessed. All EAE clinical score assessments were performed by observers blinded to treatment group. Statistical testing including 1-way ANOVA and student's unpaired t-tests were performed in GraphPad Prism (v.8). Restriction maximum likelihood (REML) mixed models were performed in jamovi (24) using GAMLj (v.2.0.6) to evaluate the effect of treatment and day post-induction on clinical score (25). A p-value less than 0.05 was considered significant. Mean ± standard deviation (SD) plotted in all graphs.

Results

7,8-dihydroxylfavone fails to enhance myelin repair in the cuprizone model of de- and remyelination

We have previously shown that 7-day ICV infusions of the structural peptide mimetic of BDNF, TDP6 and the partial TrkB agonist, LM22A-4 increase the level of MBP expression, the proportion of myelinated axons and myelin sheath thickness during remyelination after cuprizone-induced demyelination (13,14). To determine if DHF could mediate the same effect as a TrkB agonist in the same context (Fig. 1A), we first assessed the level of MBP immunostaining in the caudal corpus callosum (Fig. 1C). This revealed 7-day infusion of DHF during remyelination resulted in an increased percentage area of MBP immunostaining compared to infusion with the aCSF vehicle ($p=0.012$), but not when compared to the 14% DMSO vehicle ($p=0.22$; Fig. 1B). To confirm whether this increase in MBP staining was due to a pro-myelinating effect, we next performed electron microscopy (EM; Fig. 1D), comparing the proportion of myelinated axons in the caudal corpus callosum of mice that received the aCSF vehicle, to those that received DHF, but did not detect a change ($p=0.23$, Fig. 1E). However, electron dense myelin debris was more frequently observed in the caudal callosum of mice that received DHF (Fig. 1D). Collectively, both the MBP and EM analyses

indicate that 7-day ICV infusion of DHF itself does not enhance remyelination above either the infusion of aCSF or DMSO vehicles.

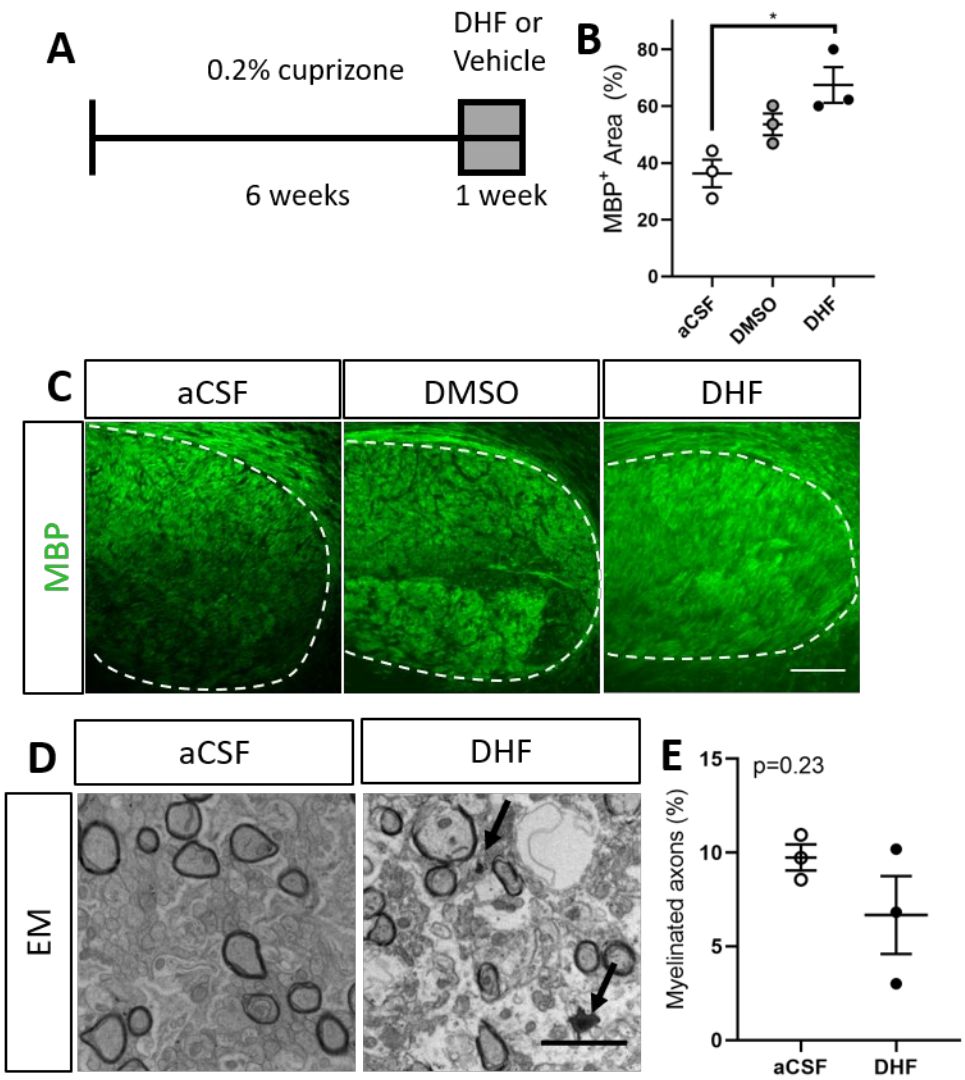

Figure 1: 7,8-dihydroxylfavone increases area of myelin basic protein (MBP) immunostaining, but not the percentage of myelinated axons during remyelination. (A) Schematic of experimental paradigm, where cuprizone demyelinated mice received either DHF, aCSF or 14% DMSO via ICV infusion for 7 days. (B) Animals receiving DHF have an increased percentage area MBP$^+$ compared to mice that received the aCSF vehicle (p=0.012) but not compared to those that received the DMSO vehicle (p=0.22, n=3/group, 1-way ANOVA, $F_{2,6}$=0.09, Tukey's post-hoc comparison). Representative (C) micrographs of MBP immunostaining (scale bar = 100um) and (D) electron micrographs in the caudal corpus callosum of aCSF, DMSO and DHF treated animals. (E) DHF treatment did not alter the percentage of axons myelinated in the caudal corpus callosum, compared to animals that received aCSF (n= 3/group, unpaired t-test, $F_{2,2}$=9.04).

7,8-dihydroxyflavone increases OPC density after cuprizone-induced demyelination

Infusion of either TDP6 or LM22A-4 for 7 days during remyelination increased the density of total $Olig2^+$ oligodendroglia in the caudal corpus callosum, primarily by increasing the density of $Olig2^+CC1^+$ post-mitotic oligodendrocytes (13,14). Here, we sought to determine if DHF, mediated the same effect by performing cell counts on sagittal brain sections triple immunolabeled for Olig2 to identify all cells in the oligodendroglial lineage, PDGFRα to identify oligodendrocyte precursor cells (OPCs) and CC1 to identify post-mitotic oligodendrocytes (Fig. 2A). This identified a trend towards an increased density of $Olig2^+$ oligodendroglia in the caudal corpus callosum of mice that received DHF treatment compared to those that received either aCSF or the DMSO vehicles (Fig. 2B). In contrast to our previous findings with TDP6 (13) and LM22A-4 (14), treatment with DHF solely increased the density of OPCs ($p=0.0002$, Fig 2C), whereas DMSO infusion did not result in a detectable difference in OPC density in the caudal corpus callosum when compared to mice treated the aCSF vehicle ($p=0.71$, Fig. 2C). There was no detectable change ($p=0.96$) in the density of $Olig2^+CC1^+$ post-mitotic oligodendrocytes in the caudal corpus callosum of mice that received DHF, compared to those that received aCSF or DMSO (Fig 2D). These data indicate that ICV infusion of DHF, but not its DMSO vehicle during the remyelinating period selectively triggers an OPC proliferation event.

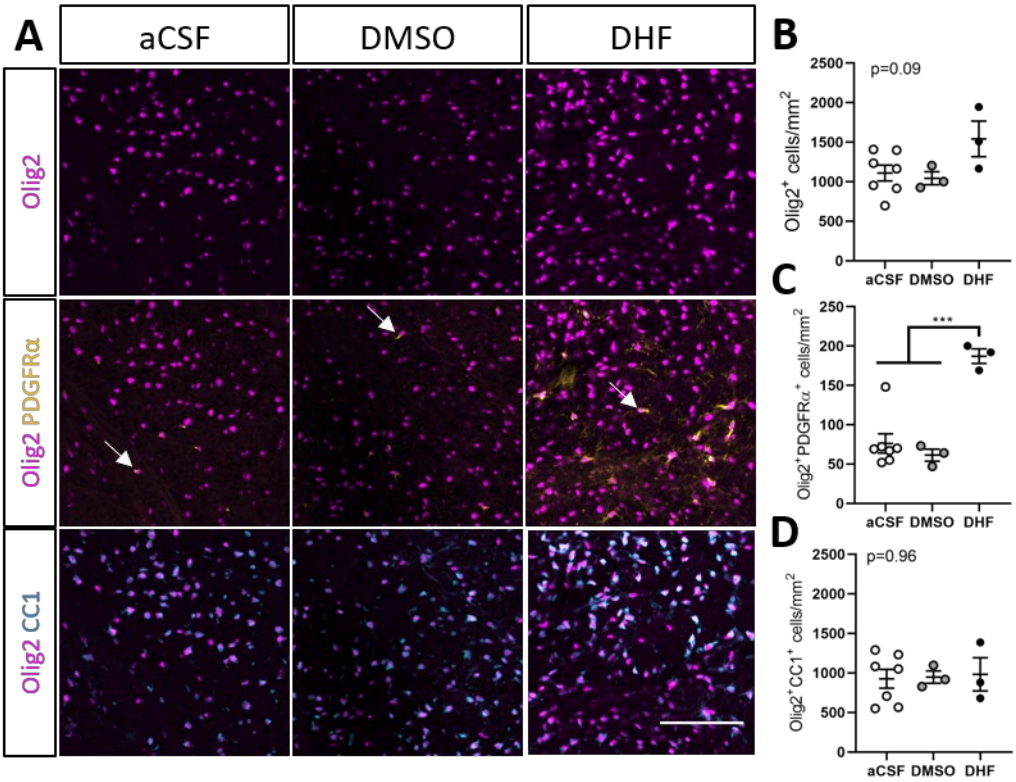

Figure 2: Increased oligodendrocyte progenitor cell (OPC) density in the caudal corpus callosum of mice treated with 7,8-dihydroxylfavone during remyelination. (A) Representative micrographs for Olig2-PDGFRα-CC1 triple immunolabelling in the cadual corpus callosum of mice treated with aCSF, DMSO or DHF during remyelination. Scale bar=100µm. Brightness and contrast have been adjusted to improve visibility. (B) The density of Olig2+ oligodendroglia demonstrated a trend increase in mice that were treated with DHF compared to those that received the aCSF and DMSO vehicles ($p=0.089$, $F_{2,10}=0.89$). This was driven by (C) an increase ($p=0.0002$, $F_{2,10}=0.16$) in $Olig2^+PDGFR\alpha^+$ OPC (arrows in A) densities in the corpus callosum of mice that received DHF compared to those that received aCSF or DMSO vehicles. (D) There was no change in the density of $Olig2^+CC1^+$ cells in the corpus callosum of mice treated with DHF compared to aCSF and DMSO ($p=0.96$, $F_{2,10}=0.77$). For (B-C) (*n*=3-7/group, 1-way ANOVA, Tukey's post-hoc comparison).

7,8-dihydroxyflavone administered directly into the CNS after onset of clinical signs does not alter the clinical course of EAE

Others have shown that daily intraperitoneal injection of DHF in DMSO from the day of EAE induction can improve its clinical course and improve neuropathological outcomes including the extent of inflammation and demyelination (15). We sought to build on these findings to determine if DHF treatment had a direct

283 effect on the CNS during EAE via ICV infusion, and if it could alter the course of EAE after the onset of
284 clinical signs (Fig. 3A). We found that compared to the treatment with DMSO vehicle, ICV infusion of DHF
285 from Day 13 when mice exhibited tail weakness and/or weakness of one hindlimb, did not alter the clinical
286 course of EAE (Treatment: $p=0.47$, Fig. 3B). Consistent with this, we also found that there remained
287 profound demyelination in the lumbar spinal cord of DHF-treated EAE at Day 35, using a combination of
288 SCoRe and Fluoromyelin staining to detect compact myelin and myelin debris (Fig. 3C). Importantly, this
289 demyelination was accompanied by an extensive infiltration of Iba1+ macrophages and/or microglia in
290 lateral myelinated tracts of the lumbar spinal cord, which were observed to contain myelin debris. Overall,
291 these results indicate that direct infusion of DHF into the CNS is unable to alter the course of EAE or
292 promote myelin repair.

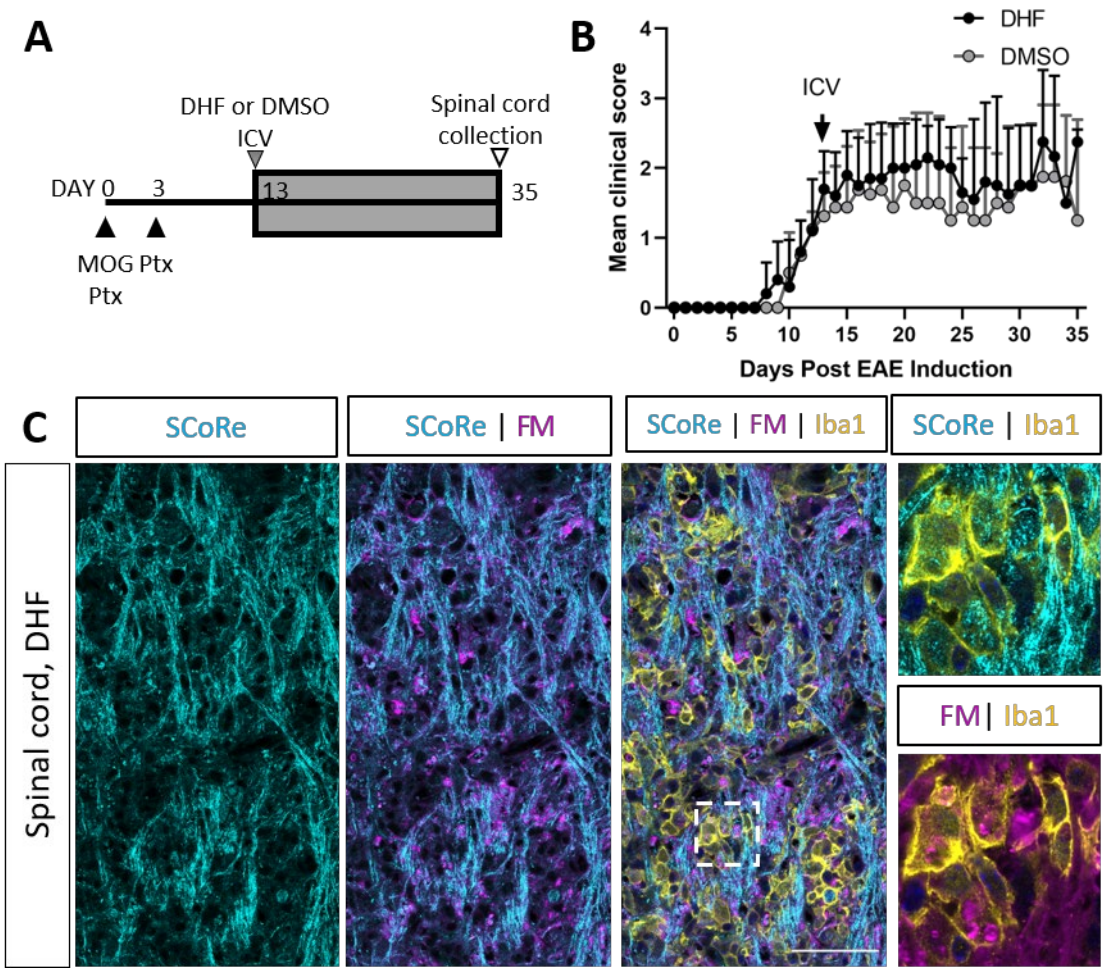

Figure 3: Direct CNS infusion of 7,8-dihydroxyflavone after the onset of clinical signs does not alter the disease course or restore myelin in EAE. (A) Schematic of experimental paradigm of EAE experiments, where ICV infusion into the CNS of either DHF or the DMSO vehicle commenced on Day 13 after the onset of tail and/or hindlimb weakness (MOG: myelin oligodendrocyte glycoprotein; Ptx: pertussis toxin). (B) There was no change (treatment effect: p=0.46) in the mean clinical score of mice that received either DHF or DMSO (n=4-5/group, mean ± SD plotted, REML mixed-effects model to test the effects of treatment and day post-EAE induction, $F_{1,7}$=0.59). (C) Longitudinal section of the lateral white matter of the lumbar spinal cord of a DHF-treated mouse at Day 35, demonstrating extensive demyelination as detected by SCoRe imaging (cyan) and fluoromyelin staining (magenta) with prevalent myelin debris both extracellularly and within Iba1$^+$ (yellow) macrophages / microglia (insets).

Discussion

Here, we sought to determine if direct infusion into the CNS of the reported TrkB agonist DHF, could promote myelin repair in two preclinical animal models of MS. We found that DHF failed to promote myelin repair in the cuprizone model of de- and remyelination, with no increase in the proportion of myelinated axons after cuprizone withdrawal compared to the aCSF treated vehicle. This was despite increases in the percentage area of the caudal corpus callosum positive for MBP staining. DHF also failed to alter the clinical course of EAE, an immune-driven model of MS, when it was administered via ICV infusion after the initial onset of tail and/or hindlimb weakness. These results directly contradict previous findings, wherein recombinant BDNF, and other compounds, TDP6 and LM22A-4, shown to activate TrkB signalling in the cuprizone model, and in multiple *in vitro* contexts (10,14,26,27), did promote remyelination by increasing the proportion of myelinated axons and/or density of post-mitotic oligodendrocytes (13,14). They also contradict findings in EAE, where intraperitoneal administration of DHF improved the clinical course, preserved myelination and reduced neuroinflammation in the spinal cord (15). Indeed, in the current study, the only indication that DHF may have pro-myelinating properties was a significant increase in OPC density in the caudal corpus callosum at the end of 7 days of remyelination.

Proliferation of OPCs is required to replace the myelinating oligodendrocytes that are killed during cuprizone induced demyelination. In this respect, the increased OPC density in response to DHF infusion during the remyelinating phase in cuprizone-demyelinated mice could be a priming event that precedes robust myelin repair that extends past the 7-day treatment period examined here. Indeed, ICV infusion of LM22A-4 also significantly increased OPC density in the caudal corpus callosum after 7-days of infusion in

cuprizone-demyelinated mice (14). However, the LM22A-4-mediated increase in OPC density was accompanied by a strong pro-differentiation effect, with a significant increase in post-mitotic oligodendrocytes and myelinated axons (14). Promoting oligodendrocyte differentiation and myelination of axons are two measures of effective myelin repair that DHF was unable to elicit, and that are characteristic of other TrkB agonists known to promote CNS myelination via oligodendroglial TrkB signalling pathways (13,14,28). More importantly, these are capabilities that are absolutely essential for a candidate remyelinating therapy for MS, in which the primary aim is to overcome arrested OPC differentiation (6,29). Further, acute increases in OPC densities typically comprise a pathologic response in multiple contexts, including other toxin-induced models of demyelination, lysolecithin and ethidium bromide lesions (30,31), as well as traumatic brain injury (32,33). This suggests that the increase in OPC density mediated by DHF could be a pathologic response, and that DHF itself may have toxic effects, particularly since animals treated with the DMSO vehicle alone did not demonstrate the same OPC increase. Similarly, while there was increased MBP staining in the DHF treated corpus callosum, there was also myelin debris present in DHF mice that was absent in the aCSF control mice. Myelin debris in response to DHF treatment also speaks to a pathologic response. Overall, the results from treating cuprizone-demyelinated mice with DHF, indicate that this reported TrkB agonist (12) is unable to promote myelin repair and is not a viable remyelinating therapeutic candidate for MS.

The poor efficacy of DHF as a therapeutic for MS when directly administered to the CNS was also demonstrated in EAE as it did not modify the clinical course or extent of demyelination and neuroinflammation. Testing potential MS therapeutics in EAE is widely considered to be required due to the complex interactions between the immune system and the CNS that occur in MS, and most disease-modifying MS treatments clinically available are immuno-modulatory and have been tested in this model (7). Previously, DHF was shown to prevent EAE from progressing beyond tail weakness when administered

352 via intraperitoneal injection from the day of EAE induction (15). This is in contrast with the strategy used
353 here, where DHF was administered directly to the CNS via ICV infusion and did not commence until EAE
354 mice demonstrated tail and/or hindlimb weakness. The timing of treatment from the onset of clinical signs
355 is more likely to represent what MS patients will experience and from this perspective it is disappointing
356 that DHF did not alter the clinical course of EAE in the current study. However, the dose of DHF used here
357 is 131x lower than the intraperitoneal delivered dose (15) and this may account for the lack of efficacy in
358 the current study. It is also possible that the ICV infusion of DHF into the cerebrospinal fluid failed to
359 reach the lumbar and sacral spinal cord which are severely affected by peripheral immune cell infiltration
360 and demyelination that precipitate the ascending paralysis characteristic of EAE. This seems highly likely
361 based on the extent of demyelination and neuroinflammation still present in the lumbar spinal cord of
362 DHF-treated EAE mice at Day 35. Therefore, it would be interesting to compare how high-dose peripheral
363 delivery of DHF from clinical onset influences the clinical course of EAE, and if this strategy would be as
364 effective as the prophylactic regime previously tested (15).

365

366 Importantly, the reduced severity of EAE in the previous study (15) and increased OPC density in cuprizone
367 in response to DHF treatment raise important questions about whether DHF is mediating these effects in
368 a TrkB-dependent manner. In EAE, it is probable that peripheral administration of DHF from the day of
369 MOG sensitisation is preventing immune-mediated demyelination and could be exerting an anti-
370 inflammatory effect. Notably, there were significantly fewer CD45+ leukocytes, CD3+ T-cells, CD20+ B-
371 cells and CD11b+ macrophages present in the spinal cord of the peripherally DHF-treated EAE mice (15).
372 The role of TrkB activation in modulating immune cell behaviours in EAE is contentious (34) with reports
373 that BDNF-TrkB signalling on autoreactive T-cells can promote their survival and propagate the
374 autoimmune attack against myelin (35). A pro-survival effect of TrkB activation on T-cells appears counter
375 to the results of DHF treatment in the previous EAE study (15), which are more aligned with the anti-

oxidant properties of DHF (17,18,36) which could attenuate neuroinflammation (37,38). It is possible that the anti-oxidant properties of DHF are what drives the therapeutic neuroprotective effects observed when it is used in other neurodegenerative disease models (39–41). Indeed, it has been shown that the anti-oxidant properties of DHF are able to promote neuronal cell line survival in a TrkB-independent manner (17,18). This is highly problematic as *in vitro* neuronal survival assays are frequently how the neurotrophic activity of candidate TrkB agonists are initially assessed (10–12,42), and it has been shown that the interaction of DHF with TrkB is dependent on the extent of neuronal maturation in these contexts (16). These past data, combined with the current results, raise the possibility of DHF having off-target effects, and call into question whether it primarily acts as TrkB agonist *in vivo*.

Similarly, the role of TrkB activation on OPC proliferation, which was the primary result of DHF treatment during remyelination after cuprizone, is controversial. There is only limited evidence from cuprizone treated BDNF HET mice, that have a 40% reduction in BDNF but the full complement of both $p75^{NTR}$ and TrkB receptors, that BDNF, and therefore potentially TrkB activation, promotes OPC proliferation after a demyelinating event (43). It could be argued that the DHF-mediated increase in OPC density was not mediated in a TrkB-dependent manner, particularly since DHF did not trigger an increase in myelinated axons or an increase in post-mitotic oligodendrocyte density; outcomes which are characteristic of oligodendroglial TrkB-mediated myelin repair after cuprizone (13,14). However, it should be noted that like LM22A-4, which also mediated an increase in OPC density after cuprizone (14), DHF is biased towards PI3K/Akt signalling (16,40) which is associated with promoting OPC survival (44,45). As the TrkB-dependency of the DHF effect was not examined in the current study using genetic or pharmacological tools, it remains possible that the increase in OPC density is TrkB dependent. This could mean that DHF, like LM22A-4 is hypothesized to, mediates TrkB-transactivation (14,46) rather than directly triggering cell surface TrkB dimerization and autophosphorylation. This is especially likely given the small molecular

weight of DHF. Importantly, both LM22A-4 and DHF have come under scrutiny for their inability to transduce TrkB signalling in a BDNF-like manner. They were among 6 reported TrkB agonists that failed to elicit TrkB phosphorylation in cortical neuron cultures after 2 hours of incubation (42). Collectively, the current data from the DHF-treated cuprizone mice, the previous study in EAE (15), and studies examining the mode of action of DHF in other contexts (16–18,36,42) suggest that DHF may not act solely via the TrkB receptor and that studies using DHF as functional BDNF-mimic to interrogate TrkB function *in vivo* should be interpreted with caution.

Conclusions

Overall, the lack of pro-myelinating effect of DHF after cuprizone induced demyelination and its failure to modify the disease course of EAE when directly administered to the CNS indicate that DHF is not a viable therapeutic candidate to promote myelin repair in MS and other demyelinating diseases. Further, the results of the current study, combined with existing literature on DHF and its mode of action, suggest that DHF may have off-target effects *in vivo*.

Acknowledgements

We thank Dr Chris Dwyer and Michele Binder (Florey Institute for Neuroscience and Mental Health) for their assistance with the experimental autoimmune encephalomyelitis (EAE) model. We acknowledge the staff and facilities of the Biological Optical Microscopy Platform (University of Melbourne), Centre for Advanced Histology and Microscopy (Peter MacCallum Centre) and Florey Advanced Microscopy and Immunohistochemistry Service.

Funding

JLF was supported by a MS Research Australia Postdoctoral Fellowship (#14-056). This work was funded by an Australian National Health and Medical Research Council Project Grant (#APP1105108) awarded to SSM. This work was supported by the Assistant Secretary of Defense for Health Affairs, endorsed by the Department of Defense, USA, through the Multiple Sclerosis Research Program W81XWH-17-MSRP-IIRA under award no. MS170031 to Junhua Xiao and Simon Murray. Opinions, interpretations, conclusions, and recommendations are those of the authors and not necessarily endorsed by the Assistant Secretary of Defense for Health Affairs or Department of Defense (USA).

Conflicts of Interest

The authors declare no conflict of interest.

References

1. Longo FM, Massa SM. Small-molecule modulation of neurotrophin receptors: a strategy for the treatment of neurological disease. Nat Rev Drug Discov [Internet]. 2013;12(7):507–25. Available from: http://www.ncbi.nlm.nih.gov/pubmed/23977697

2. Fletcher JL, Murray SS, Xiao J, Fletcher JL, Murray SS, Xiao J. Brain-Derived Neurotrophic Factor in Central Nervous System Myelination: A New Mechanism to Promote Myelin Plasticity and Repair. Int J Mol Sci [Internet]. 2018 Dec 19 [cited 2019 May 3];19(12):4131. Available from: http://www.mdpi.com/1422-0067/19/12/4131

3. Fulmer CG, VonDran MW, Stillman AA, Huang Y, Hempstead BL, Dreyfus CF. Astrocyte-Derived

BDNF Supports Myelin Protein Synthesis after Cuprizone-Induced Demyelination. J Neurosci [Internet]. 2014;34(24):8186–96. Available from: http://www.jneurosci.org/cgi/doi/10.1523/JNEUROSCI.4267-13.2014

4. Wong AW, Xiao J, Kemper D, Kilpatrick TJ, Murray SS. Oligodendroglial expression of TrkB independently regulates myelination and progenitor cell proliferation. J Neurosci [Internet]. 2013;33(11):4947–57. Available from: http://www.ncbi.nlm.nih.gov/pubmed/23486965

5. Van't Veer A, Du Y, Fischer TZ, Boetig DR, Wood MR, Dreyfus CF. Brain-derived neurotrophic factor effects on oligodendrocyte progenitors of the basal forebrain are mediated through trkB and the MAP kinase pathway. J Neurosci Res [Internet]. 2009 Jan [cited 2018 Nov 14];87(1):69–78. Available from: http://www.ncbi.nlm.nih.gov/pubmed/18752299

6. Murphy NA, Franklin RJM. Recruitment of endogenous CNS stem cells for regeneration in demyelinating disease [Internet]. 1st ed. Vol. 231, Functional Neural Transplantation IV: Translation to Clinical Application, Part B. Elsevier B.V.; 135–163 p. Available from: http://dx.doi.org/10.1016/bs.pbr.2016.12.013

7. Faissner S, Plemel JR, Gold R, Yong VW. Progressive multiple sclerosis: from pathophysiology to therapeutic strategies. Nat Rev Drug Discov [Internet]. 2019;18(12):905–22. Available from: http://dx.doi.org/10.1038/s41573-019-0035-2

8. Poduslo JF, Curran GL. No Title. 1996;36.

9. Chao M V. Neurotrophins and their receptors: a convergence point for many signalling pathways. Nat Rev Neurosci. 2003;4(4):299–309.

10. Massa SM, Yang T, Xie Y, Shi J, Bilgen M, Joyce JN, et al. Small molecule BDNF mimetics activate TrkB signaling and prevent neuronal degeneration in rodents. J Clin Invest. 2010;120(5):1774–85.

11. O'Leary PD, Hughes RA. Design of potent peptide mimetics of brain-derived neurotrophic factor. J Biol Chem. 2003;278(28):25738–44.

12. Jang S-W, Liu X, Yepes M, Shepherd KR, Miller GW, Liu Y, et al. A selective TrkB agonist with potent neurotrophic activities by 7,8-dihydroxyflavone. Proc Natl Acad Sci U S A [Internet]. 2010;107(6):2687–92. Available from: http://www.pubmedcentral.nih.gov/articlerender.fcgi?artid=2823863&tool=pmcentrez&rendertype=abstract

13. Fletcher JL, Wood RJ, Nguyen J, Norman XEML, Jun CMK, Prawdiuk AR, et al. Targeting TrkB with a Brain-Derived Neurotrophic Factor Mimetic Promotes Myelin Repair in the Brain. 2018;38(32):7088–99.

14. Nguyen HTH, Wood RJ, Prawdiuk AR, Furness SGB, Xiao J, Murray SS, et al. TrkB Agonist LM22A-4 Increases Oligodendroglial Populations During Myelin Repair in the Corpus Callosum. Front Mol Neurosci [Internet]. 2019 Aug 27 [cited 2020 Sep 23];12:205. Available from: https://www.frontiersin.org/article/10.3389/fnmol.2019.00205/full

15. Makar TK, Nimmagadda VKC, Singh IS, Lam K, Mubariz F, Judge SI V, et al. TrkB agonist, 7,8-dihydroxyflavone, reduces the clinical and pathological severity of a murine model of multiple sclerosis. J Neuroimmunol [Internet]. 2016;292:9–20. Available from: http://dx.doi.org/10.1016/j.jneuroim.2016.01.002

16. Liu X, Obianyo O, Chan CB, Huang J, Xue S, Yang JJ, et al. Biochemical and Biophysical Investigation of the Brain-derived Neurotrophic Factor Mimetic 7,8-Dihydroxyflavone in the Binding and Activation of the TrkB Receptor. J Biol Chem [Internet]. 2014 Oct 3 [cited 2016 Oct 18];289(40):27571–84. Available from: http://www.jbc.org/lookup/doi/10.1074/jbc.M114.562561

17. Han X, Zhu S, Wang B, Chen L, Li R, Yao W, et al. Antioxidant action of 7,8-dihydroxyflavone protects PC12 cells against 6-hydroxydopamine-induced cytotoxicity. Neurochem Int [Internet]. 2014 Jan [cited 2020 Dec 16];64(1):18–23. Available from: https://pubmed.ncbi.nlm.nih.gov/24220540/

18. Chen J, Chua K-W, Chua CC, Yu H, Pei A, Chua BHL, et al. Antioxidant activity of 7,8-dihydroxyflavone provides neuroprotection against glutamate-induced toxicity. Neurosci Lett [Internet]. 2011 Jul 25 [cited 2017 Mar 26];499(3):181–5. Available from: http://www.ncbi.nlm.nih.gov/pubmed/21651962

19. Skripuletz T, Gudi V, Hackstette D, Stangel M. De- and remyelination in the CNS white and grey matter induced by cuprizone: The old, the new, and the unexpected. Histol Histopathol. 2011;26(12):1585–97.

20. Baker D, Gerritsen W, Rundle J, Amor S. Critical appraisal of animal models of multiple sclerosis. 2011;17(6):647–57.

21. Wallin MT, Culpepper WJ, Campbell JD, Nelson LM, Langer-Gould A, Marrie RA, et al. The prevalence of MS in the United States. Neurology [Internet]. 2019 Mar 5 [cited 2019 Jul 25];92(10):e1029–40. Available from: http://www.ncbi.nlm.nih.gov/pubmed/30770430

22. Guyenet SJ, Furrer SA, Damian VM, Baughan TD, la Spada AR, Garden GA. A simple composite phenotype scoring system for evaluating mouse models of cerebellar ataxia. J Vis Exp [Internet]. 2010 [cited 2020 Sep 23];(39). Available from: /pmc/articles/PMC3121238/?report=abstract

23. Gonsalvez DG, Yoo S, Fletcher JL, Wood RJ, Craig GA, Murray SS, et al. Imaging and Quantification of Myelin Integrity After Injury With Spectral Confocal Reflectance Microscopy. Front Mol Neurosci [Internet]. 2019 Nov 19 [cited 2020 Sep 24];12:275. Available from:

https://www.frontiersin.org/article/10.3389/fnmol.2019.00275/full

24. Project T jamovi. jamovi (v. 1.2) [Internet]. 2020. Available from: https://www.jamovi.org

25. Gallucci M. GAMLj: General, Mixed and Generalized Models module for Jamovi [Internet]. 2020. Available from: https://gamlj.github.io/index.html

26. Schmid D a, Yang T, Ogier M, Adams I, Mirakhur Y, Wang Q, et al. A TrkB small molecule partial agonist rescues TrkB phosphorylation deficits and improves respiratory function in a mouse model of Rett syndrome. J Neurosci [Internet]. 2012;32(5):1803–10. Available from: http://www.pubmedcentral.nih.gov/articlerender.fcgi?artid=3710112&tool=pmcentrez&rendertype=abstract

27. Wong AW, Giuffrida L, Wood R, Peckham H, Gonsalvez D, Murray SS, et al. TDP6, a brain-derived neurotrophic factor-based trkB peptide mimetic, promotes oligodendrocyte myelination. Mol Cell Neurosci [Internet]. 2014;63:132–40. Available from: http://dx.doi.org/10.1016/j.mcn.2014.10.002

28. Geraghty AC, Gibson EM, Ghanem RA, Greene JJ, Ocampo A, Goldstein AK, et al. Loss of Adaptive Myelination Contributes to Methotrexate Chemotherapy-Related Cognitive Impairment. Neuron [Internet]. 2019 Jul 20 [cited 2019 Jul 11];103(2):250-265.e8. Available from: https://linkinghub.elsevier.com/retrieve/pii/S0896627319303897

29. Chang A, Tourtellotte WW, Rudick R, Trapp BD. Premyelinating Oligodendrocytes in Chronic Lesions of Multiple Sclerosis. N Engl J Med [Internet]. 2002 Jan 17 [cited 2020 Dec 15];346(3):165–73. Available from: https://pubmed.ncbi.nlm.nih.gov/11796850/

30. Gensert JM, Goldman JE. Endogenous progenitors remyelinate demyelinated axons in the adult CNS. Neuron. 1997;19(1):197–203.

31. Levine JM, Reynolds R. Activation and proliferation of endogenous oligodendrocyte precursor cells during ethidium bromide-induced demyelination. Exp Neurol [Internet]. 1999 [cited 2020 Dec 14];160(2):333–47. Available from: https://pubmed.ncbi.nlm.nih.gov/10619551/

32. Flygt J, Djupsjö A, Lenne F, Marklund N. Myelin loss and oligodendrocyte pathology in white matter tracts following traumatic brain injury in the rat. Eur J Neurosci [Internet]. 2013 Jul [cited 2017 Mar 29];38(1):2153–65. Available from: http://doi.wiley.com/10.1111/ejn.12179

33. Armstrong RC, Mierzwa AJ, Sullivan GM, Sanchez MA. Myelin and oligodendrocyte lineage cells in white matter pathology and plasticity after traumatic brain injury. Neuropharmacology [Internet]. 2016 Nov [cited 2017 May 30];110(Pt B):654–9. Available from: http://www.ncbi.nlm.nih.gov/pubmed/25963414

34. Lühder F, Gold R, Flügel A, Linker RA. Brain-derived neurotrophic factor in neuroimmunology: Lessons learned from multiple sclerosis patients and experimental autoimmune encephalomyelitis models. Arch Immunol Ther Exp (Warsz) [Internet]. 2013 Apr 3 [cited 2016 Jul 11];61(2):95–105. Available from: http://link.springer.com/10.1007/s00005-012-0211-0

35. De Santi L, Annunziata P, Sessa E, Bramanti P. Brain-derived neurotrophic factor and TrkB receptor in experimental autoimmune encephalomyelitis and multiple sclerosis. J Neurol Sci [Internet]. 2009 [cited 2017 Apr 3];287(1):17–26. Available from: http://www.sciencedirect.com/science/article/pii/S0022510X09008363

36. Cho SJ, Kang KA, Piao MJ, Ryu YS, Fernando PDSM, Zhen AX, et al. 7,8-dihydroxyflavone protects high glucose-damaged neuronal cells against oxidative stress. Biomol Ther [Internet]. 2019 Jan 1 [cited 2020 Dec 16];27(1):85–91. Available from: http://www.biomolther.org/journal/view.html?doi=10.4062/biomolther.2018.202

554 37. Michaličková D, Hrnčíř T, Canová NK, Slanař O. Targeting Keap1/Nrf2/ARE signaling pathway in
555 multiple sclerosis [Internet]. Vol. 873, European Journal of Pharmacology. Elsevier B.V.; 2020
556 [cited 2020 Dec 16]. Available from: https://pubmed.ncbi.nlm.nih.gov/32017935/

557 38. AA M, J P, D B, R L, JM M, M B, et al. Tracking CNS and systemic sources of oxidative stress during
558 the course of chronic neuroinflammation. Acta Neuropathol [Internet]. 2015 [cited 2020 Dec
559 16];130(6). Available from: https://pubmed.ncbi.nlm.nih.gov/26521072/

560 39. Jiang M, Peng Q, Liu X, Jin J, Hou Z, Zhang J, et al. Small-molecule TrKB receptor agonists improve
561 motor function and extend survival in a mouse model of huntington's disease. Hum Mol Genet.
562 2013;22(12):2462–70.

563 40. Wu C-H, Hung T-H, Chen C-C, Ke C-H, Lee C-Y, Wang P-Y, et al. Post-Injury Treatment with 7,8-
564 Dihydroxyflavone, a TrkB Receptor Agonist, Protects against Experimental Traumatic Brain Injury
565 via PI3K/Akt Signaling. Ohno M, editor. PLoS One [Internet]. 2014 Nov 21 [cited 2016 Oct
566 21];9(11):e113397. Available from: http://dx.plos.org/10.1371/journal.pone.0113397

567 41. Liu C, Chan CB, Ye K. 7,8-dihydroxyflavone, a small molecular TrkB agonist, is useful for treating
568 various BDNF-implicated human disorders. Transl Neurodegener [Internet]. 2016;5(1):2.
569 Available from: http://www.translationalneurodegeneration.com/content/5/1/2

570 42. Boltaev U, Meyer Y, Tolibzoda F, Jacques T, Gassaway M, Xu Q, et al. Multiplex quantitative
571 assays indicate a need for re-evaluating reported small-molecule TrkB agonists. 2017;1670.

572 43. Tsiperson V, Huang Y, Bagayogo I, Song Y, VonDran MW, DiCicco-Bloom E, et al. Brain-Derived
573 Neurotrophic Factor Deficiency Restricts Proliferation of Oligodendrocyte Progenitors Following
574 Cuprizone-Induced Demyelination. ASN Neuro [Internet]. 2015;7(1). Available from:
575 http://asn.sagepub.com/lookup/doi/10.1177/1759091414566878

576 44. Ebner S, Dunbar M, McKinnon RD. Distinct roles for PI3K in proliferation and survival of
577 oligodendrocyte progenitor cells. J Neurosci Res [Internet]. 2000 Nov 1 [cited 2019 May
578 6];62(3):336–45. Available from: http://www.ncbi.nlm.nih.gov/pubmed/11054802

579 45. Ness JK, Mitchell NE, Wood TL. IGF-I and NT-3 Signaling Pathways in Developing
580 Oligodendrocytes: Differential Regulation and Activation of Receptors and the Downstream
581 Effector Akt. Dev Neurosci [Internet]. 2002 [cited 2019 May 6];24(5):437–45. Available from:
582 http://www.ncbi.nlm.nih.gov/pubmed/12666655

583 46. Lee FS, Chao M V. Activation of Trk neurotrophin receptors in the absence of neurotrophins. Proc
584 Natl Acad Sci U S A [Internet]. 2001 Mar 13 [cited 2017 Apr 3];98(6):3555–60. Available from:
585 http://www.ncbi.nlm.nih.gov/pubmed/11248116

586

587

588 **Supplementary Figure**

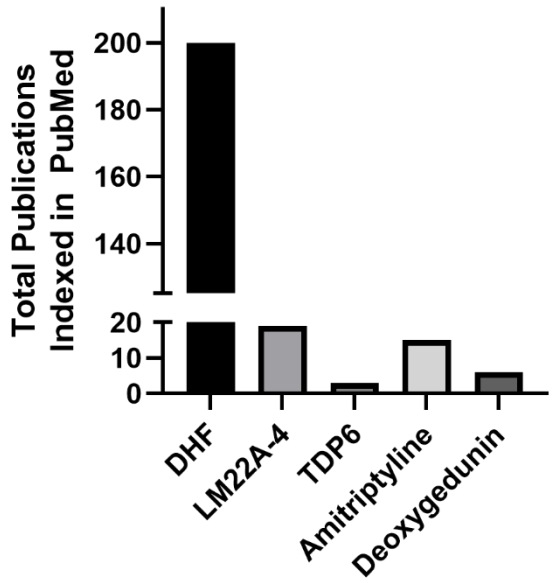

589

590 **Fig. S1: Total number of publications for each TrkB agonist indexed in PubMed**. Each TrkB agonist was
591 used as a search term in PubMed and the 'results by year' were downloaded and summed. Note for DHF
592 and Amitriptyline TrkB was included as an additional search term and only publications since their
593 characterisation as partial TrkB agonists were used (ie. from 2010 for DHF and 2007 for amitriptyline).
594 Search date: 12 April 2021.